Astron. Astrophys. 357, 920–930 (2000)

ASTRONOMY AND ASTROPHYSICS

Preliminary spectroscopic analysis of the "spotted" roAp star HD 83368 in the Li I 6708 Å region⋆

N.S. Polosukhina[1], A.V. Shavrina[2], M. Hack[3], V. Khalack[2], V. Tsymbal[4], and P. North[5]

[1] Crimean Astrophysical Observatory (CRAO) (polo@crao.crimea.ua)
[2] Main Astronomical Observatory of National Academy of Sciences, Ukraine, Kiev 252650, Ukraine (shavrina,khalack@mao.kiev.ua)
[3] Department of Astronomy, Trieste University, Via Tiepolo 11, 34131 Trieste, Italy (hack@ts.astro.it)
[4] Tavrian National University, Yaltinskaya st.4, Simpheropol 330000, Ukraine (VAD@ccssu.crimea.ua)
[5] Inst. d'Astronomie, Univ. Lausanne, 1290 Chavannes-des-Bois, Switzerland (Pierre.North@obs.unige.ch)

Received 25 May 1999 / Accepted 20 March 2000

Abstract. The preliminary determination of the atmospheric chemical composition of the Li "spotted" roAp star HD 83368 has been obtained by the synthetic spectrum method. The locations of two lithium spots are determined by the procedure of "mapping", based on the Doppler line shifts for different rotation phases.

Key words: stars: abundances – stars: chemically peculiar – stars: individual: HD 83368 – stars: magnetic fields – stars: starspots

1. Introduction

All the information concerning the Li abundance in stellar atmospheres is extremely important for testing the stellar internal structure and evolution theory. In fact Li is destroyed in the internal stellar layers because of nuclear reactions of lithium with hydrogen at relatively low temperatures of about two million degrees, and surface Li dilution occurs because of convective motions. Hence the presence of lithium in the stellar spectra is the evidence of slowed circulation between the external cool layers and the internal hot ones. The interpretation of the observed lithium abundance in the stellar atmospheres is one enigma of astrophysics. In fact, until the present time the physical processes responsible for the variety in the abundance of this element among stars with similar physical parameters, are not clear.

During the evolution along the main sequence, a normal star with noticeable initial lithium abundance is expected to lose it due to the fragility of the Li nucleus and to various mechanisms of mixing, and to come to the end of its evolution having almost fully exhausted the reservoir of this element. However, among the evolved stars (red giants) large differences of lithium abundance have been observed. This fact shows that in the process of evolution, there are not only processes of lithium destruction, but other possible causes, which brake this Li depletion. In the cases of large lithium abundance, various hypotheses about lithium synthesis were suggested (Wallerstein & Conti, 1969). The magnetic field may be one of the causes, braking the mixing of star matter and the convective motions. Therefore in the papers of Wallerstein & Conti (1969), Wallerstein & Sneden (1982) and of Lambert & Ries (1981), and Lambert & Sawyer (1984) it is hypothesized that the Li-rich giants in their evolution changes have passed the stage of chemically peculiar star with magnetic field and that lithium synthesis is the result of a spallation reaction, which takes place on the stellar surfaces with strong magnetic fields, which would accelerate protons and alpha particles.

With respect to the lithium abundance in chemically peculiar stars there are some contradictory data (Faraggiana et al., 1996; Hack et al., 1997). The chemically peculiar stars possess unusual individual characteristics, first of all, such chemical anomalies as high abundances of heavy elements, particularly of rare elements, rather strong magnetic fields, non homogeneous distribution of chemical elements on the stellar surface. The method of Doppler imaging, applied to some stars, shows that chemical anomalies are distributed in spots or rings, connected apparently with the magnetic field structure (Hatzes, 1991). Some of the roAp stars are characterized by non-radial pulsations on time scales of minutes to tens of minutes (Kurtz, 1990). The large range of the lithium line intensity in the spectra of CP stars (Faraggiana et al., 1996; Hack et al., 1997) is evidence of the complexity of the physical nature of these stars. Until now there has been no theory which can explain this phenomenon, assuming that the 6708 Å feature can indeed be interpreted as the Li I doublet, rather than as an unidentified line of some strongly overabundant rare earth element. Although spallation reactions in local flashes on the stellar surface have been suggested, this idea has never been thoroughly developed. On the other hand, the radiative diffusion theory (Babel & Michaud 1991a, 1991b) seems successful in explaining the abundance anomalies of many species, though no specific study on Li in Ap stars has been published. Since Li is mostly ionized in these

Send offprint requests to: A.V. Shavrina

⋆ Based on observations collected at the European Southern Observatory, La Silla, Chile

Table 1. List of observations. Spectral range: A = 6675-6735 Å, B = 6120–6180 Å, C = 6615–6670 Å.

Sp. #	Date d.m.y.	UT h m	Exp. [m]	HJD 2450000	Phase (rotat.)	Range
04[a]	8. 3.96	4 05	90	150.705	-	A
23	10.3.96	4 41	20	152.705	0.331	A
38	11.3.96	5 11	20	153.726	0.689	A
48	12.3.96	6 15	20	154.770	0.055	A
57	13.3.96	0 25	20	155.527	0.320	B
61	13.3.96	4 19	20	155.690	0.378	A
65	13.3.96	4 44	20	155.707	0.384	A
71	13.3.96	7 02	30	155.807	0.419	A
77	14.3.96	0 50	20	156.545	0.678	A
83	14.3.96	6 23	30	156.779	0.760	A
85	14.3.96	6 57	30	156.803	0.768	C

[a] HD 101065 (Przybylski's star), $v \sin i = 0$ km s^{-1} (Cowley & Mathys, 1998)

stars, it is expected to sink into the deep atmospheric layers, because its electronic structure is, then, similar to that of He, an element known – and predicted – to be deficient in the atmospheres of Ap stars. On the other hand, Babel (1993) suggested that ambipolar diffusion of hydrogen may cause Li enrichment near the magnetic poles, but unfortunately no detailed study of this possibility was published.

To clarify the problem of the identification of the 6708 Å feature and answer the question of the diversity of the Li abundances among Ap stars (if the 6708 Å feature is indeed due to Li), it is necessary to increase the number of spectroscopic observations in the Li line regions. The high resolution echelle spectrographs and CCD cameras allowing high S/N ratios, the modern methods of spectral analysis (atmospheric models and computations of synthetic spectra), the use of refined atomic data, especially for rare earth elements, give the possibility to study in more detail than ever before, the spectrum in the regions of the Li lines and thus to approach the solution to this problem.

In most of the works connected with lithium observations, the resonance lithium doublet at 6708 Å is used and, very rarely, the 6103 Å line, which is in the wing of a strong Fe II line. To observe the lines of neutral lithium is difficult; usually its abundance is not large, because Li I is easily ionized (the ionization potential $\Theta_{\rm ion} = 5.39$ eV). The neutral lithium can be observed only in the surface layers of the stellar atmospheres. Besides, the resonance doublet at 6708 Å is the isotopic blend of ^{6}Li and ^{7}Li. For most stars the isotopic ratio $R = {}^6\mathrm{Li}/{}^7\mathrm{Li}$ is small, $R < 0.10$ (Andersen et al., 1984).

The first results of the observations of the roAp star HD 83368 in the spectral region of Li I 6708 Å, in the frame of the international project "Lithium in the chemically peculiar stars", were presented in the paper of North et al. (1998). In this paper the detailed description of the observations, obtained at ESO with the CAT telescope in 1996, and the interpretation of the profile changes of Li I 6708 Å with the rotational phase by the "spotted" star model, are given (see Table 1 and Fig. 1 and Fig. 2 of the quoted paper). In the present paper we continue the analysis of the spectra of this star, assuming that the 6708 Å feature can be attributed to Li I, which seems probable according to Polosukhina et al. (1999). This work is the first attempt to analyse the physical properties of HD 83368, using the method of spectral synthesis for the atmospheric model. HD 83368 is the best photometrically studied example of rapidly oscillating Ap star, belonging to the SrCrEu peculiarity type with $T_{\rm eff} = 7670 \pm 500$ K and with radius $R_\star = 2.13 \pm 0.32 R_\odot$ (North et al., 1998). The effective magnetic field changes in intensity with an amplitude of ± 737 G (Mathys, 1991). Mathys yields for this star a very high value for the quadratic magnetic field - 11 kG (Mathys, 1995; Mathys & Hubrig, 1997). The star has a single mode of pulsation. The maximum photometric amplitude of the pulsations occurs when a magnetic pole is located on the line of sight; therefore, the interval between two maxima of pulsation corresponds to half of the rotation period $P_{\rm rot} = 2\overset{\rm d}{.}851976$.

2. The photometric data

HD 83368 is a double system. The magnitude of the main component is $V = 6\overset{\rm m}{.}28$ and its mass is $M_{\rm a} = 1.95 M_\odot$ (North et al., 1998). According to the Bright Star Catalogue (Hoffleit & Jaschek, 1982), the brightness difference between the components $\Delta V = 2\overset{\rm m}{.}4$. Hurly & Warner (1983) have obtained UBV photometry for the resolved components: $V(A) = 6\overset{\rm m}{.}25, B-V = 0\overset{\rm m}{.}25, U-B = 0\overset{\rm m}{.}12$ and $V(B) = 9\overset{\rm m}{.}09, B-V = 0\overset{\rm m}{.}64, U-B = 0\overset{\rm m}{.}15$. The angular separation of the components $d_{\rm p}$ is $3''.1$ (Hoffleit & Jaschek, 1982) and Hipparcos parallax of 0.01380 arcsec yields the distance of the system equal to 72 pc. The minimum orbital period of the system is $P_{\rm orb} = 657$ years, and the variation of the radial velocity due to the orbital motion is less than 0.01 km s^{-1} in one year. In their paper Kurtz et al. (1997) show that the possible variations of the Doppler shift due to the orbital motion are as small as $\Delta\lambda = 10^{-7}$ Å. It is important to remember these values for the analysis of the spectral observations, obtained at various phases.

3. Variability of the mean longitudinal magnetic field

The analysis of the Ap stellar spectra is usually complicated, due to the overabundances of some chemical elements, which are probably connected with the magnetic field structure. As it has been noted above, HD 83368 was very carefully studied by photometry (Kurtz, 1990; Kurtz et al., 1997) and also a large number of magnetic field measurements were carried out. Mathys (1995) has determined the values of the quadratic magnetic field, which is a function of the effective field $H_{\rm eff}$ and of the surface one $H_{\rm s}$.

One of the problems of this work is the necessity to take into account the Doppler shift effects due to the non-homogeneous stellar surface distribution of the chemical elements and the effects of the magnetic intensification of some spectral lines. Special attention was given to the lithium line 6708 Å, and also to the lines of other elements with high values of Landé factor. The

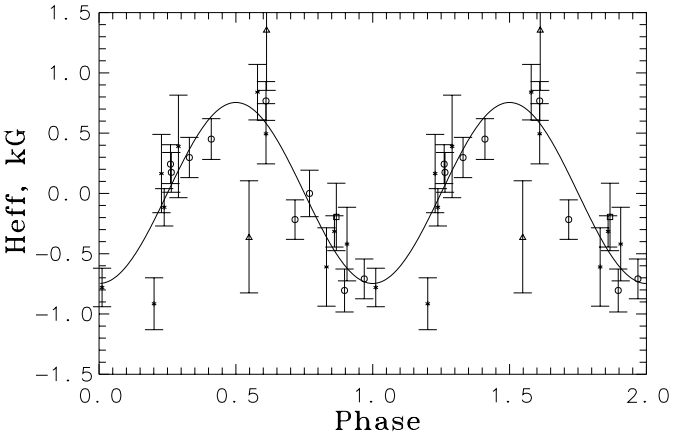

Fig. 1. The best curve fitting the observed longitudinal magnetic field variations (by the least square method, Eq. (4). The Thompson's data (Thompson, 1983) are indicated by circles and Mathys's data (Mathys, 1991) by asterisks, (Mathys & Hubrig, 1997) by squares, and the excluded data of Mathys (1991) by triangles. Vertical bars indicate the errors of the measurements.

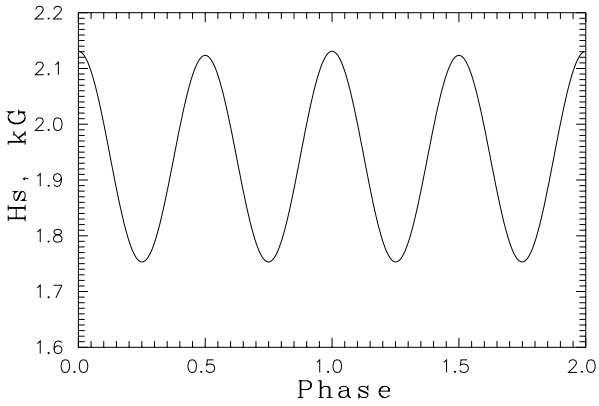

Fig. 2. Variation of the mean surface magnetic field with the rotational phase of HD 83368 calculated for $i = 89°, \beta = 74°$ and $H_{\rm p}$ = 2730 G.

magnetic field geometry in Ap stars is often characterized by the parameter $r = H_{\rm eff}(min)/H_{\rm eff}(max)$, where $-1 \le r \le 1$ (Hensberge et al., 1977). For most of the Ap stars, the variation of the mean longitudinal magnetic field observed throughout the rotation cycle appears nearly sinusoidal:

$$\langle H_{\rm eff}\rangle = H_0 + H_1 \cos\alpha, \tag{1}$$

where α is the angle between the line of sight and the axis of the magnetic field. Spherical geometry gives for $\cos\alpha$ the following exspression:

$$\cos\alpha(\phi) = \cos i\cos\beta - \sin i\sin\beta\cos 2\pi(\phi+\phi_0), \tag{2}$$

where β and i are the angle of inclination of the rotational axis to the axis of the magnetic field and to the line of sight respectively, and ϕ is the rotational phase. When $\phi + \phi_0 = 0$, we have the minimum value of angle α and consequently the maximum value of longitudinal magnetic field. It is easy to see that

$$\tan i\tan\beta = (1-r)/(1+r). \tag{3}$$

For HD 83368, supposing a pure dipolar configuration of the magnetic field, Mathys (1991) has performed a least-squares fit of the values of $\langle H_{\rm eff}\rangle$ previously observed by Thompson (1983) through H_β photopolarimetry, and measurements of $\langle H_{\rm eff}\rangle$, obtained by Mathys in 1985, 1987 and 1988, with the Eq. (1). The fitted parameters are $H_0 = 22 \pm 28\ G, H_1 = 737 \pm 84\ G$ and $\phi_0 = 0.343 \pm 0.013$, which give us $r = -0.94 \pm 0.29$. In the case of an oblique rotating magnetic dipole, the relation of the mean longitudinal magnetic field to the polar field strength $H_{\rm p}$ is proportional to $\cos\alpha$ (Hensberge et al., 1977)

$$\langle H_{\rm eff}\rangle = H_{\rm p}\frac{15+u}{20(3-u)}\cos\alpha, \tag{4}$$

where u is the limb-darkening coefficient. Matthews et al. (1996) have derived the limb-darkening coefficient for HD 83368 directly from the observed ratio of pulsation amplitudes in the optical (Strömgren *vby* and Cousins RI) and IR (JHK) bandpasses supposing $T_{\rm eff} \approx 8000\ K$. For the spectral range, with central wavelength $\lambda_{\rm c} = 6200$ Å (this wavelength corresponds to Mathys' observations), a value of $u \approx 0.32$ has been derived, that was used in our calculations (see Eq. (4) and Eq. (5)). By varying the parameters i and β, which define the angle α at a given rotational phase (see Eq. (2)), we have performed a least-squares fit of the available values of $\langle H_{\rm eff}\rangle$ (excluding the two measurements published by Mathys (1991) for one night in 1986 near $\phi = 0.6$ with huge estimated errors) to the Eq. (4) with minimization of the discrepancies between the calculated and observed values of $\langle H_{\rm eff}\rangle$ (see Fig. 1). By this method we have obtained an estimate of the polar magnetic field strength $H_{\rm p} = 2730 \pm 280\ G$ with fit goodness $\chi^2 = 1.37$ and parameters $i = 89° \pm 16°, \beta = 74° \pm 10°, \phi_0 = 0.332 \pm 0.013$, that are in good agreement with the data of Mathys (1991) and Kurtz (1990). Last parameters were used in order to construct the variability of the mean surface magnetic field modulus, averaged over the full visible stellar disk versus the rotational phase for a pure dipolar configuration (Hensberge et al., 1977):

$$H_{\rm s} = H_{\rm p}\tfrac{3}{3-u}\{\ (0.77778 - 0.22613u)\cos^2\alpha + (0.64775 - 0.23349u)\sin^2\alpha\}, \tag{5}$$

where u is the same as in Eq. (4). The variation of $H_{\rm s}$ with the phase ϕ is shown in Fig. 2.

It must be emphasized, that the mean surface magnetic field modulus for HD 83368 determined in such a way does not correspond to the recent estimate of the mean quadratic magnetic field $\sqrt{\langle H_{\rm eff}^2\rangle + \langle H_{\rm s}^2\rangle}$ = 11 kG by Mathys (Mathys, 1995, Mathys & Hubrig, 1997). The mean quadratic magnetic field is diagnosed from the second-order moment of the unpolarized line profile (about the line centre), $R_{\rm I}^2(\lambda_0) = \frac{1}{W_\lambda}\int r_{\rm I}(\lambda - \lambda_0)(\lambda-\lambda_0)^2\ d\lambda$, where the integration was carried out over the whole width of the observed line. Here W_λ is the equivalent width and $r_{\rm I}$ is the unpolarized line profile. This moment characterizes the unpolarized line width, that includes the constant part (natural width, rotational and thermal Doppler broadening, instrumental profile, etc.) and the part variable with ϕ, which is proportional to the mean quadratic magnetic field. But, if we suppose that some lines under analysis are generated in the

"abundance spots" on the stellar surface, then the line broadening due to the stellar rotation also would vary with ϕ and will not be constant as supposed by Mathys (1995). Consequently this evaluation of the mean quadratic magnetic field could be significantly greater than our estimation of the mean surface magnetic field modulus.

4. Analysis of the spectra

Spectral observations were performed at ESO with the 1.4m Coudé Auxiliary Telescope (CAT) and the Coudé Échelle Spectrometer (CES). The detector was ESO CCD #34 with 2048 pixels along the direction of dispersion (the pixels are $15\,\mu m \times 15\,\mu m$ wide). Table 1 details the observations, i.e. time, phase and wavelength coverage. The resolving power for all spectra was $R = 100000$ (resolution at 6705 Å: 67.1 mÅ) and signal-to-noise ratio was S/N = 100 to 120.

Fig. 3 shows the variability of the Li I feature; it shows the spectra, as well as the equivalent width and radial velocity of each of the two components of this feature. The quantitative analysis of the spectrum of this star in the regions 6675–6735 Å, 6120–6180 Å and 6615–6675 Å, to our knowledge, is carried out for the first time. In Fig. 4 the normalized spectrum in the region of the lithium blend 6708 Å for the rotational phases 0.055 and 0.419 is shown. The variability of the spectral lines, which change both their position (shift of the line as a whole) and the profile appearance, is evident. These changes are the largest and impressive for the lithium blend 6708 Å. The other lines, in particular 6690.9 Å, 6706.7 Å, 6727.7 Å also reveal some variability. Apparently we observe surface abundance variability not only of lithium, but of other elements too, connected with different geometry and probably physical conditions in the spots and in the non-spotted photosphere.

The quantitative analysis of the spectra of HD 83368 was carried out by the method of synthetic spectra with the help of Tsymbal's code STARSP (Tsymbal, 1994) and Kurucz's atmospheric models (Kurucz, 1993). We used the Kurucz line lists (Kurucz, 1995, CDROM 23) and the VALD list (Piskunov et al., 1995, Kupka et al., 1999), accessible on INTERNET (URL *http://cefa-www.harvard.edu/amdata/ampdata/kurucz23/sekur.html* and *http://www.astro.univie.ac.at/ vald*, respectively). The data for the doubly ionized rare earth element (REE) were taken from the list of Reader & Corliss (1980). For Nd III, Pr III, Ce II and Ce III we used the level energy data and gf data provided to us by Cowley (1998), Bord (1998) from Michigan University and by Sugar (1998) from NIST (National Institute of Standards and Technologies). For identification purpose we have also calculated the positions of the lines of the ionized rare elements using the energy level data of NIST (URL *http://www.aeldata.nist.gov*) and, for Dy III, the energy levels from the paper of Spector et al. (1997). Due to the small observed spectral region and the insufficient covering of rotation phases we carried out only a preliminary analysis. We have tried to determine the mean chemical composition (in the photosphere and spots) for each observed rotational phase,

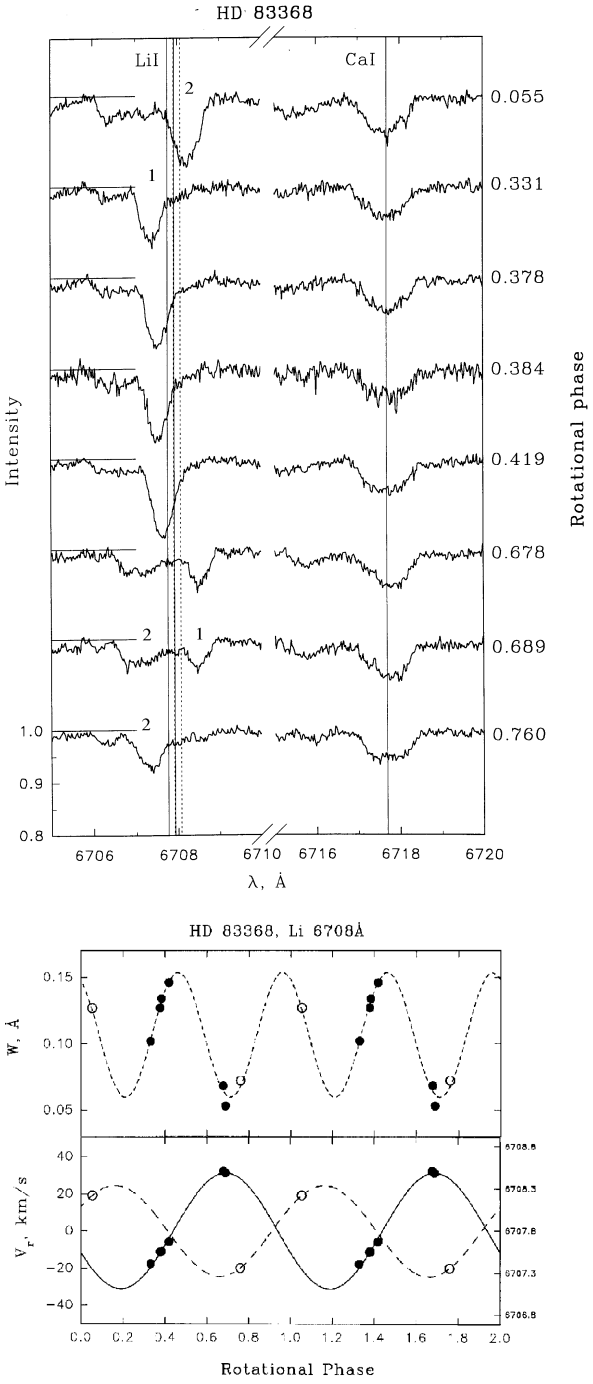

Fig. 3. Spectra of the star HD 83368 made in 1996 in residual intensity scale (North et al., 1998). The rotational phases are given on the right. At the left side of each spectrum, the position of the continuum is shown. The lines due to spot 1 and spot 2 are indicated. Below: lithium line equivalent width and radial velocity variation for the two spots: dark circles - spot N 1, open circles - spot N 2.

using one atmospheric model with $T_{\rm eff} = 7750\ K, \log g = 4.0$ and metal abundance [M/H]=0.0. The calculated spectra were convolved with the rotation profile with the value of $v \sin i = 34\ km\ s^{-1}$. This and other parameters for the calculations of the synthetic spectrum were chosen in accordance

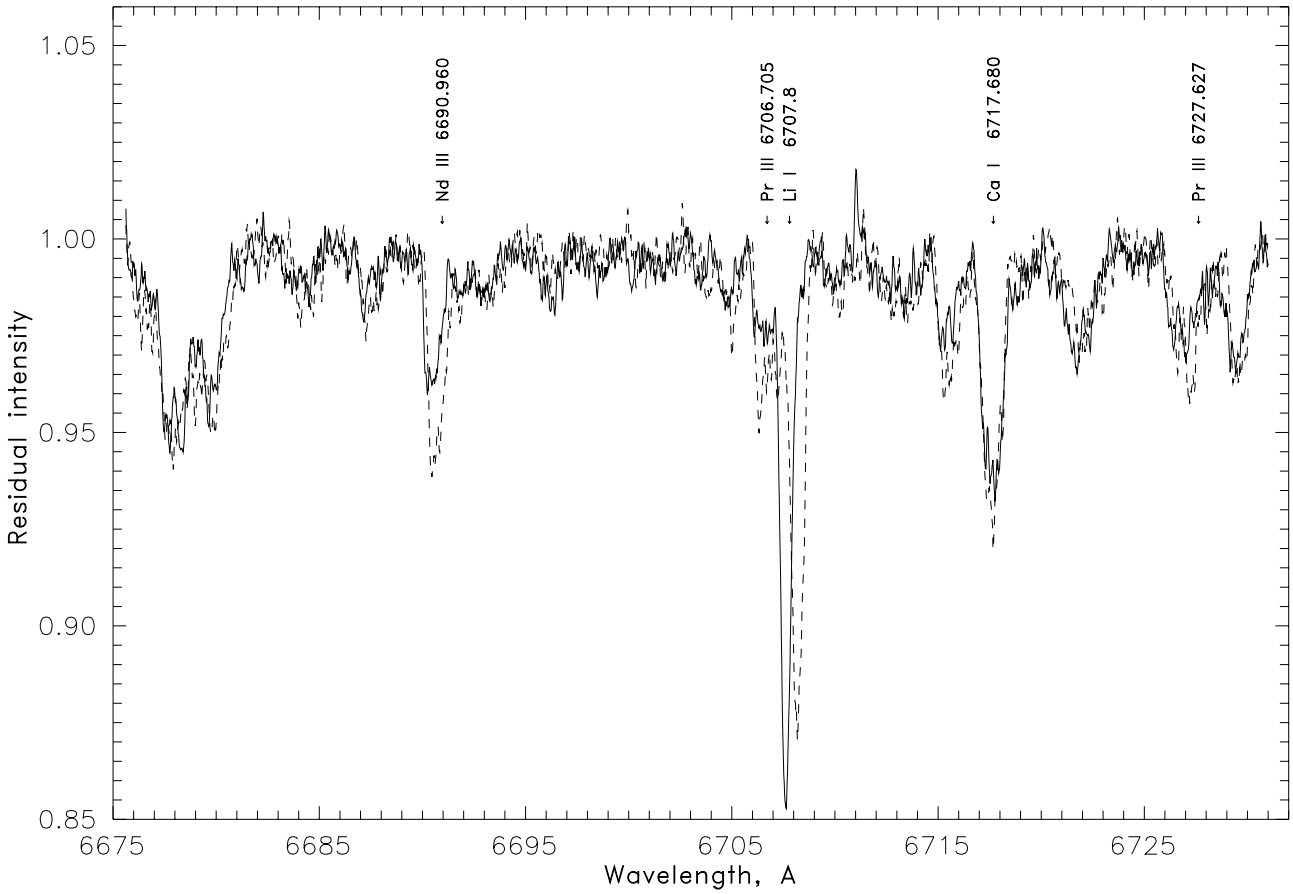

Fig. 4. The comparison of two spectra of HD 83368 at the phases 0.419 and 0.055 nearest to the maximum and minimum respectively of the longitudinal magnetic field. Continuous line: the spectrum for phase 0.419; dashed line: for phase 0.055. In the last spectrum the lines of Nd III and Pr III are remarkably enhanced.

with the data of North et al. (1998). We also tried to calculate the synthetic spectra with other model atmospheres, changing $T_{\rm eff}$ on $\pm 250\ K$ and $\log g$ on ± 0.5. The best agreement in the abundances computed from Fe I and Fe II lines was achieved for the model $T_{\rm eff} = 7750\ K, \log g = 4.0$. By fitting the calculated synthetic spectra with the observed ones we have found line intensity changes for several elements, depending on the rotational phase.

The values of $\log N$ relative to hydrogen for the different phases are given in Table 2 (Columns 2 to 10). The number of lines used for abundance estimate and the errors for each element are given in Columns 11 and 12 of Table 2. Let us note that the estimated errors on the abundances depend mainly on the line intensities, numbers of lines, blending with other lines, accuracy of gf-values and inhomogeneous surface distribution of the element (and of other elements, due to blending), and therefore depend on the rotation phase too. Because of these difficulties we give only one estimated value of the error for all phases. The procedure of fitting observed and calculated spectra was carried out until the discrepancy for all the analysed lines of each element reached its minimum. The last three columns of Table 2 give, for comparison, the solar abundances (Kurucz, 1993) and the abundances for a similar roAp star, HD 24712, by Ryabchikova et al. (1997). HD 24712 also shows variability of chemical composition versus the rotational phase, but has no measurable Li 6708 Å line. We notice that the abundances and their behaviour for the majority of the elements (Fe, Ca, REE, light elements) are essentially similar to the case of HD 83368. The data for the light elements (C,N,O) in HD 24712 were taken from the paper of Roby & Lambert (1990).

- For neutral iron, which shows small abundance variations with phase ($\log N = -4.6$ to -4.9), such errors were estimated as 0.1 dex. For Fe II ($\log N$ = –4.3 to –4.7), it was estimated to 0.2 dex. A more reliable value of the abundance of Fe II, taking into account the Zeeman line splitting, was obtained only for the phase 0.320 (λ 6120–6178 Å) from the lines 6147 Å and 6149 Å, giving $\log N = -4.6 \pm 0.1$. Some variability of abundance with rotational phases was also shown by other elements of the iron group: Ti II (–6.8 to –7.3), Cr I (–4.1 to –5.0) and Co I (–5.5 to –6.3).
- The noticeable excesses of abundances in the atmosphere of this CrSrEu star relative to the solar ones were shown by Cr I (1.4 to 2.3 dex), Y I (2.8 to 3.4 dex), Ba II (0.9 dex) and by rare earths (2.0 dex on the average, see Table 2). Y and Ba are s-process elements like Sr, but no Sr lines are present in the spectral regions studied here.

Table 2. The element abundances for each rotation phase from the spectral range 6675–6735 Å.

Phase	0.055	0.320	0.331	0.378	0.384	0.419	0.678	0.689	0.760	N	error	Sun		
Sp, No	48	57[a]	23	61	65	71	77	38	83	lines	(dex)	Kurucz,	HD 24712	
El	max[b]					max[b]						1993	min[b]	max[b]
1	2	3	4	5	6	7	8	9	10	11	12	13	14	15
C	-3.8		-4.0	-4.5	-4.2	-4.0	-4.2	-3.9	-4.4	6	0.3	-3.48	-4.5	
N	-3.1		-4.0	-3.8	-3.6	-3.0	-3.3	-3.2	-3.5	10	0.3	-3.99	-4.4	
O		-3.4	-4.3		-3.7	-4.0			-4.4	2	0.3	-3.11	-3.8	
Na		-6.1								2	0.3	-5.71		
Al	-6.6		-6.5	-6.6	-6.0	-6.3	-6.4	-6.1	-6.0	1	0.2	-5.57	-5.53	
Si	-4.0	-4.9	-4.1	-4.1	-4.0	-3.9	-4.1	-4.2	-4.2	5	0.2	-4.49	-4.43	
S		-5.2								5	0.3	-4.83		
Ca I	-5.2	-5.6	-5.5	-5.5	-5.5	-5.3	-5.2	-5.1	-5.6	2	0.1	-5.68	-5.69	
Ca II		-5.3					-5.8	-5.8		3	0.3		-5.22	-4.88
Ti II	-7.2		-6.8	-7.3	-6.9	-6.9	-7.1	-7.1	-7.3	2	0.2	-7.05	-7.22	-7.29
Cr I	-4.1	-5.0	-4.9	-4.4	-4.5	-4.4	-4.4	-4.3	-4.6	4	0.2	-6.37	-5.93	-5.80
Cr II	-4.4			-4.3	-4.2	-4.6				4	0.3		-5.58	-5.33
Fe I	-4.6	-4.9	-4.8	-4.7	-4.8	-4.7	-4.7	-4.8	-4.8	4	0.1	-4.37	-4.77	-4.88
Fe II	-4.5	-4.7	-4.6	-4.4	-4.3	-4.7	-4.4	-4.5	-4.6	10	0.2		-4.80	-5.11
Co I	-6.3	-5.5				-5.6	-6.0		-6.2	1	0.3	-7.12	-5.88	-5.57
Y I	-6.4	-6.4	-7.0	-6.6	-6.7	-6.6	-6.4	-6.6	-7.0	4	0.2	-9.80	-7.80	-7.80
Ba II		-9.1								1	0.2	-9.91	-9.12	-8.98
La II	-8.5		-9.0	-8.7	-8.6	-8.8	-8.6	-8.4	-9.2	3	0.4	-10.82	-9.40	-8.75
Ce II	-8.1		-8.6	-8.4	-8.2	-8.6	-8.6	-8.3	-8.7	2	0.3	-10.49	-9.18	-8.90
Pr II		-9.3								4	0.3	-11.33	-10.15	-9.60
Pr III	-8.5	-8.8	-9.1	-8.9	-8.6	-8.9	-8.5	-8.6	-8.9	2	0.3			
Nd II	-8.5	-9.3	-9.0	-8.8	-8.6	-8.6	-8.2	-8.4	-8.8	4	0.3	-10.54	-9.13	-8.64
Nd III	-7.2	-7.8	-8.0	-7.8	-7.8	-7.6	-7.3	-7.4	-7.8	1	0.3			
Sm II	-8.5		-9.1	-8.6	-8.4	-8.7	-8.7	-8.7	-8.6	3	0.3	-11.04	-9.75	-9.16
Eu II		-9.8							-9.8[c]	1	0.3	-10.53	-9.50	-9.00
Gd II	-8.9			-8.5	-8.4	-8.6	-8.9	-8.9	-8.6	6	0.3	-10.92	-9.11	-8.70
Er II	-8.6		-8.6	-8.5	-8.5	-8.3	-8.6	-8.1	-8.2	1	0.3	-11.11	-9.79	-9.53
Lu II		-9.2								1	0.3	-11.28		

[a] from spectral range 6120–6180 Å;
[b] these phases corespond to the maximum (minimum) of stellar magnetic field;
[c] this estimate was obtained from line 6645.06 Å in the phase 0.768, nearest to 0.760.

- We made an attempt to determine ourselves the value of the magnetic field from the line profiles of Fe II 6147 Å and 6149 Å (Fig. 5). We have computed the profiles of these lines taking into account the magnetic splitting for two values of the magnetic field: 2 kG, calculated by us as described in Sect. 2, and 11 kG (taking into account the Paschen-Back effect, see Mathys, 1995; Mathys & Hubrig, 1997). The calculated Fe II line profiles in Fig. 5a correspond to the flux from whole visible stellar surface with a homogeneous abundance. For a magnetic field strength of 2 kG, we can get a much better fit to the observe spectra when we assume that the surface of the star is covered with Fe II spots at $l_1 = 110°$ and $l_2 = 170°$ and Pr II spot at $l = 100°$ (where l is longitude in spherical coordinates relative to the observer) - see Fig. 5b. For a field strength of 11 kG, we did have to exclude the Fe II spot at $l_2 = 170°$ and Pr II spot in order to get reasonable agreement (we used only one main spot of Fe II with $l_1 = 110°$, the nearest to the centre of visible hemisphere of star for this phase 0.320, i.e. $115.2°$). However, the fit for a 2 kG field is still much better suggesting that the field strength is indeed closer to 2 kG than to 11 kG.
- Abundance variability with the rotational phase was found also for the light elements: C I (–3.8 to –4.5), N I (–3.0 to –4.0), O I (–3.4 to –4.4). The more reliable value for O I is probably $\log N = -3.4$, obtained in the region 6120–6180 Å from some O I lines near 6156–6158 Å for the phase 0.320. The analysis of two weak O I lines in the lithium region (6726.28 Å and 6726.54 Å) is difficult due to the blending with the Ca II line 6726.06 Å, the intensity of which also changes with the phase. The Ca I abundance change is (–5.1 to –5.6) with an error of 0.1 dex.
- For the phase 0.055, corresponding to the passage of one of the lithium spots through the central meridian (in this phase the spot is near the centre of the visible hemisphere), we have found the maximum abundances of N I (–3.1), Cr I (–4.1), Fe I (–4.6) and most of the rare earth elements (see Tables 2).

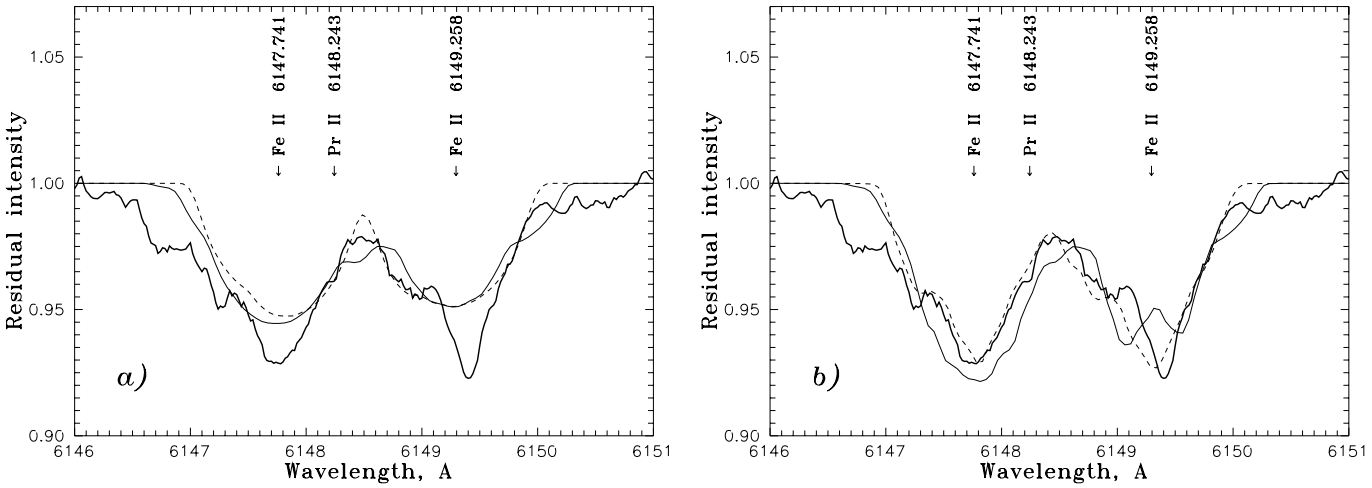

Fig. 5. **a** The calculated profiles of Fe II 6147.74 Å and 6149.26 Å lines with the magnetic splitting. Continuous thick line: observed spectrum for the phase 0.320, dashed line: the calculated one for the field of 2 kG (Zeeman splitting), and thin line: for the field of 11 kG (Paschen-Back effect). Both spectra were calculated assuming a homogeneous surface abundance. **b** The comparison of the observed and calculated spectra for Fe II with taking into account surface spot structure of star (see Sect. 6.1). Also, dashed line - for 2 kG and thin continuous line - for 11 kG.

The phase 0.419, nearest to the central position of the other lithium spot, does not show strengthening of some rare earth elements lines (see Fig. 4 for Nd III and Pr III lines and Tables 2).

5. The rare earth elements (REE)

Special attention was paid to the line identification, taking into account the lines of the rare earths, in the computation of the synthetic spectrum especially in the region of Li 6708 Å. This kind of work is yet to be completed, but some preliminary results permit us to assign some earlier unidentified lines to rare earth elements, once- and twice-ionized. For instance, we have identified the feature 6690.96 Å as a Nd III line and two features, 6706.70 Å and 6727.67 Å, with Pr III lines. The intensities of these three lines vary, like the lithium blend, but with some phase shift relative to the latter. So, in Fig. 4 we show the spectra at two phases, nearest to the maxima of the surface magnetic field: 0.419 when the Li line has maximum intensity, and 0.055, in which all three lines of REE mentioned above are intensified. The line 6690.9 Å is possibly a blend of Nd III 6690.96 Å, Er II 6690.00 Å and Ca I 6691.02 Å. The appearence of its profile depends on the phase. We note the difference from the Li line profiles which have constant width at various phases, a fact which indicates the constant size of the Li line forming region (two spots). On the contrary, since the width of the rare earth element lines changes, then the sizes of the visible part of their abundance patches changes too.

Besides 8 spectra in the lithium region near 6708 Å we have 2 additional spectra: in the region 6120–6180 Å (phase = 0.320) and in the region 6610–6670 Å (phase = 0.768). For the last phase we see two components of the line Eu II 6645.06 Å (Fig. 6). Also two components with different intensities are observed in the Ba II, Nd III and Fe II lines (Fig. 7) for the phase 0.320. We have calculated the line profile of Eu II 6645.06 Å

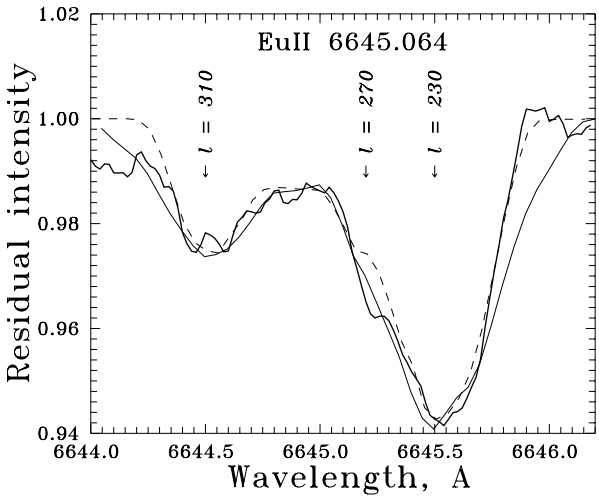

Fig. 6. The line profile of Eu II 6645.06 Å. Bold line: the observed spectrum at the phase 0.768, dashed line: the calculated one with magnetic splitting for the field of 2 kG (Zeeman splitting), and thin line for 11 kG (Paschen-Back effect), both with taking into account spot structure.

with magnetic splitting for the field of 2 kG and 11 kG, taking into account spot structure (see Table 3 in the Sect. 6).

The similar intensity ratios of the components for Fe II and Ba II at phase 0.320 indicate a similar spot (or ring) distribution of these ions near the poles with the lithium spots. The Nd III line 6145.07 Å shows an opposite intensity ratio of the two components at the same phase - probably the surface distribution of this ion differs from that of Fe II and Ba II (Fig. 7). Although the Nd III line 6145.07 Å is blended with Fe II line 6145.610 Å, the last one affects the shape of its profile insignificantly.

For computing the synthetic spectra we used the relative line strengths of Pr III from the list of Sugar (1974), and the absolute values of gf were assigned assuming equal abundances from Pr III and Pr II. For Pr II the data of Kurucz (1993) were used.

The Pr abundance, determined in the region 6120–6180 Å at phase 0.320, gives a good agreement between the calculated and the observed lines of Pr II and Pr III in the lithium region at phase 0.331. For two lines of Nd III, 6145.07 Å and 6690.96 Å, belonging to the same multiplet, we have computed the relative strengths, supposing the L-S moment sum rule. Accepting the value $\log gf = -1.328$ for the line 6145.07 Å (Cowley & Bord, 1998), we have found for the line 6690.96 Å a value $\log gf = -2.50$, that is closed to data of Bord -2.29 ± 0.20 (Bord, 1998) for this line. Using these gf values, we have obtained the same Nd abundance for the nearest phases 0.320 (line 6145.07 Å) and 0.331 (line 6690.96 Å). However this Nd abundance gives too strong intensities for the lines of Nd II (see Fig. 7), computed with the gf data from Kurucz (1993). The disagreement between the abundances derived from Nd II and Nd III consists in 0.8–1.5 dex. Similar enhanced Pr III abundances were obtained using the new values of $\log gf$ computed by Bord for four lines of Pr III: 6160.24 Å (–0.827), 6161.22 Å (–0.728), 6706.70 Å (–1.285), 6727.63 Å (–3.289). Probably, the differences in the abundances of once- and twice-ionized rare earth elements are connected with the specific conditions of ionization near the magnetic poles.

6. The lithium line profiles 6708 Å at different rotational phases

The numerous attempts to reproduce the lithium line profile suggest that two different ways can be followed. In the first way we adjust the local effective temperature of a near-polar lithium spot, assuming a given lithium abundance. The calculations show that it is necessary to strongly decrease the temperature (to 6000 K), even assuming a maximum lithium abundance $\log N = -8.80$ (3.2 in the scale of N(H) = 12.0, i.e. the initial abundance, before lithium is depleted). But so large temperature difference between the photosphere and the spots ($\Delta T_{\rm eff} \sim 1600\ K$) does not agree with the small photometric variability of the star.

The other way is the assumption of lithium stratification in the stellar atmosphere and its concentration in the surface layers, which can be provided by the mechanism of ambipolar diffusion (Babel, 1993).

If we assume that the brightness variations are synchronous with the rotation of the star, we can put definite limitations on possible differences between the physical conditions in the spots and in the photosphere. For HD 83368 the spot structure must be in accordance with the fact, that the B and V light curves are in opposite phases. We know three possible ways to explain a variation of the star brightness when a spot appears on the visible hemisphere:

1. Different spot temperature in the spot compared with that of the surrounding photosphere. Considering the dependences of theoretical B and V colours (Kurucz, 1993, CDROM 13) on $T_{\rm eff}$ (for $\log g = 4.0$) it is shown that this assumption can not explain the changes of brightness in the two colours simultaneously.
2. The most frequently used hypothesis, in the case of Ap stars, is that the spot and the atmosphere have different metallicities. But the dependence of the theoretical B and V colours (from Kurucz atmospheric models) on metallicity (for $T_{\rm eff} = 7750\ K$ and $\log g = 4.0$) indicates that the metallicity gradient may provide the observed variation in opposite phase only if the metal abundances in the photosphere and in the spot are equal to [0.5] and [1.0] respectively. However, our spectral analysis does not give so high metal abundances: the iron abundance in the photosphere of HD 83368 is, on the contrary, slightly lower than the solar one.
3. Non homogeneous (spotted) surface distribution of rare earth elements can explain the variation of B-V by REE blocking-backwarming effects with very small temperature difference between spot and photosphere (see for example, Iliev, 1983).

Therefore we accepted this third hypothesis of identical temperature conditions for the spot regions and the photosphere assuming enhanced lithium abundance in the spots.

6.1. *Line profile calculations for rotating stars with spotted surfaces*

The star rotation results in broadening all spectral lines in the stellar spectrum because of the Doppler effect. The degree of this broadening depends on the projection of the equatorial velocity on the line of sight $v \sin i$.

For calculating the lithium line profile we splitted the visible hemisphere of the star surface in 32×32 points with rectangular coordinates $(x_{\rm i}, y_{\rm i})$, each of which is the Gaussian (quadrature) division point. The line profile in this case can be calculated according to Tassoul (1978).

Let $I(x, y; \lambda - \lambda_{\rm c})$ be the intensity of radiation emitted by the point (x, y) on the disk of a non-rotating star in the spectral line at the distance $\lambda - \lambda_{\rm c}$ from the central wavelength $\lambda_{\rm c}$. For a rotating star it is necessary to use $\lambda_{\rm c} - (\lambda_{\rm c} V_{\rm z}/c)$, where $V_{\rm z}$ is the radial velocity in the point (x, y) and c the velocity of light. Since $V_{\rm z} = -xV_{\rm e} \sin i$ (where V_e is the equatorial velocity of the star, and i is the inclination angle of the rotational axis to the line of sight), the intensity of the radiation emitted by the point (x, y) on the disk of a uniformly rotating star is given by $I(x, y; \lambda - \lambda_{\rm c} - \lambda_{\rm c} x (V_{\rm e}/c) \sin i)$, and the line profile is calculated accordingly

$$\mathbf{r}(\lambda - \lambda_{\rm c}) = \frac{\int\limits_{-1}^{1} dx \int\limits_{0}^{(1-x^2)^{\frac{1}{2}}} I[x, y, \lambda - \lambda_{\rm c} - \lambda_{\rm c} x (\nu_{\rm e}/c) \sin i] dy}{\int\limits_{-1}^{1} dx \int\limits_{0}^{(1-x^2)^{\frac{1}{2}}} I_0(x, y) dy}, \qquad (6)$$

where $I_0(x, y)$ is the intensity of the continuous radiation, emitted by the point (x, y), and $I(x, y)$ is the line intensity, which is computed for each point of the visible surface taking into

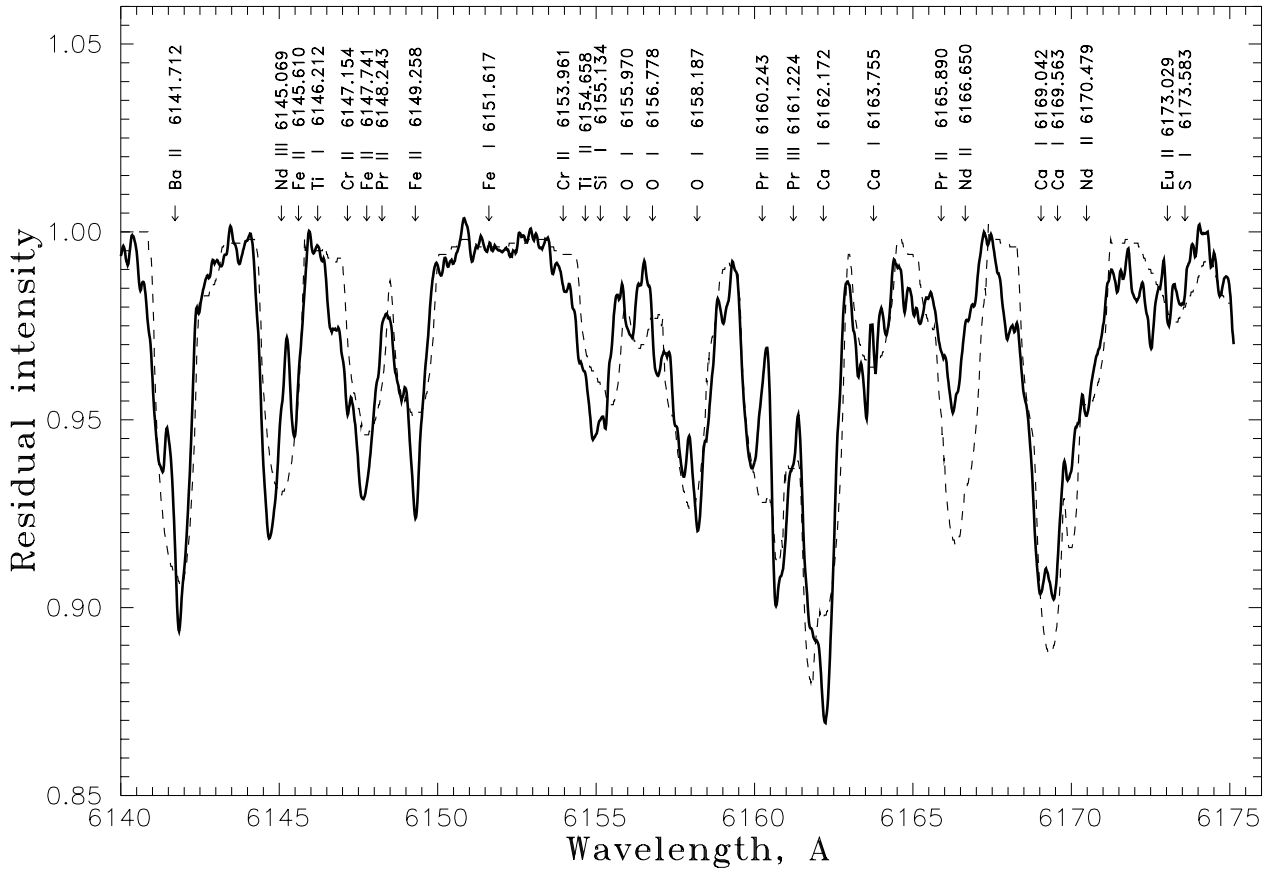

Fig. 7. The spectrum of HD 83368 in the region 6140–6175 Å. Continuous line: the observed spectrum at phase of 0.320; dashed line: the computed spectrum using Kurucz model atmosphere with $T_{\rm eff} = 7750\ K, \log g = 4.0, [M/H] = 0.0$. The spectrum has been convolved with a rotation profile for $v \sin i = 34\ km\ s^{-1}$. It is evident the splitting of the Ba II 6141.71 Å and Nd III 6145.07 Å. If we adopt the Nd abundance from the line Nd III 6145.07 Å, we obtain enhanced intensities of Nd II lines in the calculated spectrum relative to the observed spectrum.

account the presence of spots with different chemical compositions. In this work we assume there are two symmetrical circular spots with a homogeneous abundance of the selected chemical element (in this case lithium) inside the spot. The coordinates and the radius of each spot are given in spherical coordinates relative to the observer (longitude l and latitude φ).

6.2. The analysis of the Li line profiles

In the paper of North et al. (1998) it was shown the presence of two diametrically opposite spots. In this work we have calculated the coordinates and surface areas of spots supposed them as circular. The best method to reveal the spotted structure of a stellar surface is the following: spot parameter retrieval from the line profiles for a number of rotational phases. However this method demands the availability of high quality spectra, distributed over a larger number of rotational phases (more than ten), than we have. Therefore we have used the reverse method, i.e. direct spectrum modelling with choice of spot parameters in order to obtain the best fit to the observed spectra.

After clearing up questions, connected with the differences of physical conditions in the spots and its surrounding photosphere (see above), our free parameters are:

- the angle of inclination of the rotational axis to the line of sight (i);
- the equatorial velocity of rotation ($v_{\rm e}$);
- the number of spots;
- the coordinates (l, φ) and size (R) of each spot;
- the abundances of the chemical element (Li) studied in each spot.

The choice of the parameters is made in order to provide the best agreement between the theoretical and observed spectra.

To derive the spots locations we set as a first approximation the longitudes of the two spots to the points where RV curve of the Li line crosses the value of the mean radial velocity of the star. Then, changing the value of i with the spots' latitudes equal to zero, we find the best agreement between the computed and observed profiles of the Li line for all phases. A further improving of the fit we reached by varying the latitudes and minute corrections of abundances. In general a good fit was reached for phases near subsolar position of a spot, while worse one for a spot location near a limb. The procedure of fitting observed and calculated spectra was carried out until the discrepancy of both spectra reached its minimum. The variations of the parameters in the whole range of possible values permit

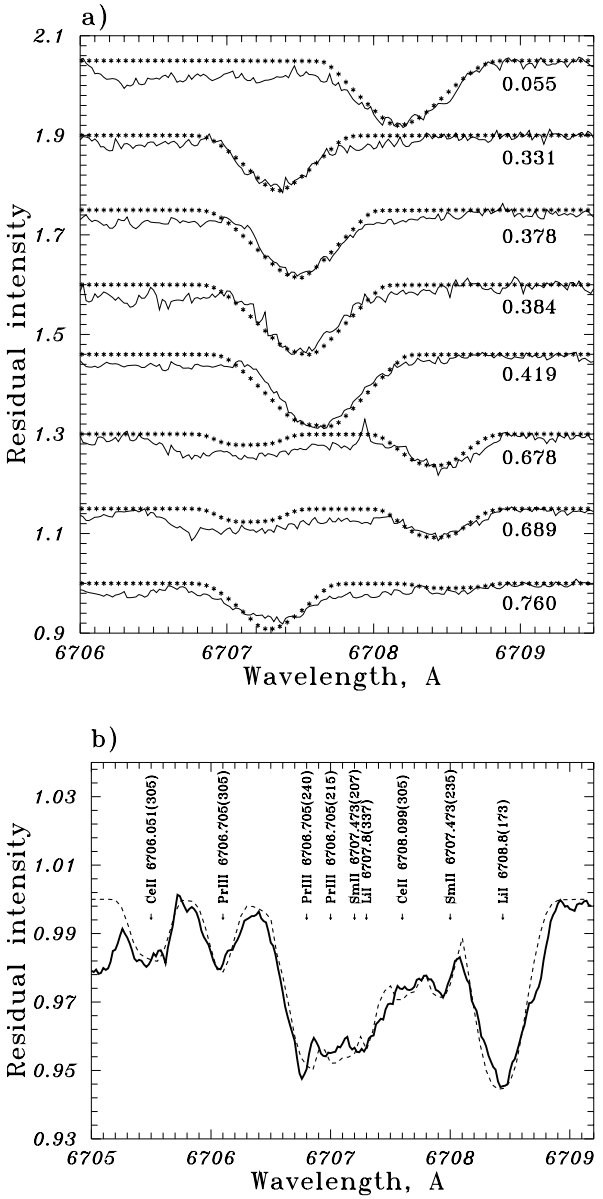

Fig. 8. a The observed and theoretical spectra for 8 rotational phases with the following parameters for the spots: spot 1: $l = 173^\circ, \varphi = 0^\circ, R = 33.5^\circ$ (near the phase 0.419), $\varepsilon_{\rm Li} = -8.4$. spot 2: $l = 337^\circ, \varphi = 0^\circ, R = 35^\circ$ (near the phase 0.055), $\varepsilon_{\rm Li} = -8.5$; **b** Calculated and observed spectrum for the phase 0.689. Four REE ions lines are involved in the calculation (see Table 3).

us to obtain a single solution for the atmospheric model with $T_{\rm eff} = 7750\,K, \log g = 4.0, i = 90^\circ, v_{\rm e} = 35\ km\ s^{-1}$ and photospheric Li abundance $\varepsilon_{\rm Li} = -10.2$,

- spot 1: $l = 173 \pm 6^\circ, \varphi = 0 \pm 6^\circ, R = 33.5 \pm 6^\circ, \varepsilon_{\rm Li} = -8.4 \pm 0.2$;
- spot 2: $l = 337 \pm 6^\circ, \varphi = 0 \pm 6^\circ, R = 35 \pm 6^\circ, \varepsilon_{\rm Li} = -8.5 \pm 0.2$.

Fig. 8a shows observed and calculated with these spot parameters the Li line profiles for all phases. In the calculations we included 10 components of the Li line fine structure for a magnetic field value, corresponding to each phase. But the influence of magnetic splitting for $H_{\rm s} \sim 2$ kG on Li abundance is insignificant ($<$0.1 dex). We used our abundance estimates for Fe and other electron-contributors elements, which differ from the solar one. The choice of these abundances affects essentially the Li estimate, because lithium is mainly ionized (Li II) in a A-type stellar atmosphere.

We also have calculated the Li profile taking into account the nearest rare earth elements lines, namely 6706.051 Å Ce II, 6706.705 Å Pr III, 6707.473 Å Sm II and 6708.099 Å Ce II. The gf-value for the last line, $\lg gf$ = –2.210, was estimated from the spectrum of Przybylski's star HD 101065, using two nearby lines of Ce II 6704.524 Å and 6706.051 Å with known gf-values. The Kurucz' atmospheric model with $T_{\rm eff} = 6750\ K, \lg g = 4.0$ and [M/H] = 0. was used for this star. We can note that Ce II lines are stronger than the Li line, in the spectrum of the Przybylski star, unlike HD 83368.

Fig. 8b shows the spectrum at phase 0.689, where we see both Li spots and the rare earth lines are rather strong. If Li spot locations have been computed for all phases together, the REE spot location were chosen for each phase independently. Our calculations for all the 8 phases confirm the hypothesis that rare earth elements may be concentrated in rings around the lithium spots. So, if lithium spots, as it was determined from the mapping procedure, belong on the equator at longitudes l = 337° and 173°, rare earths are seen on l = 20° to 60°, 100° to 155°, 195° to 240° and 275° to 325°.

Note, that we varied the Li spot latitudes, but the best results were found under zero latitudes. For REE (and Fe II spots, Sect. 4) we have adopted the same latitudes. It should be noted also that our analysis of the REE spots for all phases reveals the same features at adjacent phases. The data about the rare earth spots (or rings), visible at the phase 0.689 (see Fig. 8b), are given in the Table 3.

Table 3. Data about REE spots taken into account for the calculated spectra at Fig. 8b (phase=0.689) and at Fig. 6 (phase=0.768).

El, λ_{lab}, Å	λ_{obs}, Å	Longitude, l_{sp}	Radius, R_{sp}	$\log N_{El}$, dex
Phase = 0.689 (248°.04)				
Ce II	6705.5	$305 \pm 10^\circ$	$30 \pm 10^\circ$	-8.5 ± 0.3
6706.051	6706.1	$240 \pm 10^\circ$	$10 \pm 10^\circ$	-8.1 ± 0.3
Ce II	6707.6	$305 \pm 10^\circ$	$26 \pm 10^\circ$	-8.5 ± 0.3
6708.099	6708.0	$250 \pm 10^\circ$	$15 \pm 10^\circ$	-8.2 ± 0.3
Pr III	6706.1	$305 \pm 10^\circ$	$15 \pm 10^\circ$	-8.8 ± 0.3
6706.705	6706.8	$240 \pm 10^\circ$	$30 \pm 10^\circ$	-8.5 ± 0.3
	6707.3	$195 \pm 10^\circ$	$15 \pm 10^\circ$	-8.0 ± 0.3
Sm II	6707.6	$235 \pm 10^\circ$	$20 \pm 10^\circ$	-8.2 ± 0.3
6707.473	6708.0	$207 \pm 10^\circ$	$20 \pm 10^\circ$	-7.8 ± 0.3
Phase = 0.768 (276°.48)				
Eu II	6644.5	$310 \pm 10^\circ$	$40 \pm 10^\circ$	-9.8 ± 0.3
6645.064	6645.2	$272 \pm 10^\circ$	$15 \pm 10^\circ$	-8.9 ± 0.3
	6645.5	$228 \pm 10^\circ$	$27 \pm 10^\circ$	-8.9 ± 0.3

7. Discussion

The abundance analysis of the roAp star HD 83368 was carried out for the first time. We note again that our spectra are limited in spectral range and in number of rotational phases, therefore our abundance estimates can only have a preliminary character.

- Our calculation of the surface magnetic field H_s shows that the Li I line intensity changes in phase with H_s (Fig. 2 and 3b) and the profile depends on the position of the magnetic poles on the visible hemisphere. The insignificant offset between H_s and radial velocity of the Li line can be explained by a small offset between the centre of Li spots and magnetic poles (see Polosukhina et al., 1999).
- Analysis of the behaviour of the Li I line with the rotational phase has allowed us to compute the size of the spots, their position on the star as well as their lithium abundance. The remaining disagreements between model and observed spectra can probably be explained by more complicated spot structure than two homogeneous circular (not necessarily opposite) spots, as we have assumed.
- Special attention was given to search for the third REE spectrum - Pr III and Nd III. It appears that these lines are rather strong (in comparison with Pr II and Nd II lines) and have a more complicated surface distribution than lithium. Possibly they form rings or groups of spots. For studying them new spectra and calculations including magnetic splitting of lines of rare earth ions are necessary.
- We are forced to recognize that some of our abundance estimates (in particular for La II, Ce II, Gd II, Er II) are only upper limits due to the line weakness of these elements and the possibility of blending with other weak unidentified lines. The great uncertainty is also due to the complex spot distribution of rare earth elements, as we see from our preliminary analysis.
- The main problem of our research was initially the identification of the variable spectral feature at 6708 Å with the Li I line. New results from the observations of some roAp stars give additional indirect evidence for the identification of the line 6708 Å with the resonance doublet of Li I (Polosukhina et al., 1999).
- The research of Li problem in roAp stars is continuing. The work for reproducing the profile of the lithium blend with more thorough consideration of the lines of rare earth elements (probably their oxide's molecular lines also) and determination of the ratio ^{6}Li/^{7}Li is planned.

Acknowledgements. We are grateful to S. Sergeev for SPE code for spectra analysis, to Ch. Cowley for numerous consultations and for sending us the rare earth element data, to M. Ya. Orlow for discussing our work, to D. Bord and Ja. Sugar for suggestions and facilities to use their data. The data from Kurucz's CDROM 23, ADC NASA, VALD, NIST, were used and we thank the administrations of these databases, obtainable through INTERNET.

References

Andersen J., Gustafsson B., Lambert D.L., 1984, A&A 136, 65
Babel J., 1993, In: Dworetsky M.M., Castelli F., Faraggiana R. (eds.) Peculiar versus normal phenomena in A-type and related stars. ASP Conf. Ser. 44, p. 458
Babel J., Michaud G., 1991, A&A 241, 493
Babel J., Michaud G., 1991, A&A 248, 155
Bord D., 1998, private communication
Cowley Ch.R., 1998, private communication
Cowley Ch.R., Bord D.J., 1998, In: Brandt J.C., Ake T.B. (eds.) ASP Conf. Ser. vol. 143, p. 346
Cowley Ch.R., Mathys G., 1998, A&A 339, 165
Faraggiana R., Gerbaldi M., Delmas F., 1996, Ap&SS 238, 169
Hack M., Polosuchina N.S., Malanushenko V., Castelli F., 1997, A&A 319, 637
Hatzes A.P., 1991, MNRAS 253, 89
Hensberge H., van Rensbergen W., Goossens M., Deridder G., 1977, A&A 61, 235
Hoffleit D., Jaschek C., 1982, The bright star catalogue. 4th rev. ed., Yale Univ. Obs., 472 p.
Hurly P., Warner B., 1983, MNRAS 202, 761
Iliev I., 1983, Comm. Spec. Astrophys. Obs. USSR No. 39, 5
Kupka F., Piskunov N.E., Ryabchikova T.A., Stempels H.C., Weiss W.W., 1999, A&AS 138, 119 (VALD-2)
Kurtz D.W., 1990, ARA&A 28, 607
Kurtz D.W., van Wyk F., Goberts G., et al., 1997, MNRAS 287, 69
Kurucz R.L., 1993, CDROM 13, CDROM 23
Kurucz R.L., 1995, Harvard-Smithsonian Center for Astrophysics, Preprint No. 4080
Lambert D., Ries L., 1981, ApJ 248, 228
Lambert D., Sawyer S., 1984, ApJ 283, 192
Mathys G., 1991, A&AS 89, 121
Mathys G., 1995, A&A 293, 746
Mathys G., Hubrig S., 1997, A&AS 124, 475
Matthews J.M., Wehlau W.H., Rice J., Walker G.A.H., 1996, ApJ 459, 278
North P., Polosukhina N., Malanushenko V., Hack M., 1998, A&A 333, 644
Piskunov N.E., Kupka F., Ryabchikova T.A., Weiss W.W., Jeffery C.S., 1995, A&AS 112, 525 (VALD-1)
Polosukhina N.S., Kurtz D., Hack M., et al., 1999, A&A 351, 283
Reader J., Corliss Ch.H., 1980, Line Spectra of the Elements. ADC NASA, CDROM 3 (1980-1)
Roby S.N., Lambert D. L., 1990, ApJS 73, 67
Ryabchikova T.A., Landstreet J.D., Gelbmann M.J., et al., 1997, A&A 327, 1137
Spector N., Sugar J., Wyart J-F., 1997, J. Opt. Soc. Am. B, 14(3), 511
Sugar J., 1974, J. Res. Nat. Bur. Stds. 78A, 555
Sugar J., 1998, private communication
Tassoul J.-L., 1978, Theory of rotating stars. Princeton University Press, Princeton, 472 p.
Thompson I.B., 1983, MNRAS 205, 43
Tsymbal V.V., 1994, Odessa Astron. Publ. 7, part 2, 146
Wallerstein G., Conti P., 1969, ARA&A 7, 99
Wallerstein G., Sneden C., 1982, ApJ 255, 577